Finite Macro-Element Method for Two-Dimensional Eigen-Value Problems

H. Zhao[1] and Z. Shen[2]
[1]A*Star Institute of High Performance Computing, Singapore
[2]School of Electrical and Electronic Engineering, Nanyang Technological University, Nanyang Avenue, Singapore 639798
ezxshen@ntu.edu.sg

Abstract — This paper presents a finite macro-element method based on a new macro basis function constructed from the modal solutions of Helmholtz equation. Different from existing basis functions, the proposed macro basis function satisfies Helmholtz equation automatically, and it allows the use of coarse elements. As an example, the proposed method is applied to calculate the cutoff wavenumbers of waveguides, and its advantages are demonstrated.

I. Introduction

In the finite element method (FEM), the maximum element size is normally very small compared to the operating wavelength [1]. In some cases, the required maximum element size can be as small as one hundredth of the wavelength [2]. This makes the number of unknowns very large for high frequency problems and therefore the conventional finite element method can only be used for modeling electromagnetic problems of relatively small electrical size. It was shown that larger element size can be used if the order of the basis function is increased under the same accuracy [3]. However, the maximum element size allowed is still quite small in term of wavelength and the matrix size is very big as the frequency increases.

The reason behind the constraint on the element size in the finite element method might be due to the basis function used, which doesn't satisfy the Maxwell's equations. In FEM, it is assumed that the spatial variation of electromagnetic fields can be accurately represented by the polynomial basis function within the element. If the basis function doesn't satisfy the Maxwell's equations, the element size is required to be very small to minimize the errors.

In order to overcome the constraint on the element size, a new macro basis function is proposed in this work. The new basis function satisfies the Helmholtz equation automatically because it is based on the modal solutions of the Helmholtz equation, and the element size is no longer required to be a small fraction of the wavelength. The finite macro-element method is then developed based on the new macro basis function. As an example, we apply the finite macro-element method to calculate the cutoff wavelengths of canned and ridged waveguides. Through this example, the advantages of the proposed method are demonstrated.

II. The Macro Basis Function

Consider the two-dimensional transverse electric case of a closed waveguide problem. The Helmholtz equations governing the normal magnetic field can be written as

$$\frac{\partial^2 H_z}{\partial x^2}+\frac{\partial^2 H_z}{\partial y^2}+k_c^2 H_z=0 \tag{1}$$

where k_c is the cutoff wavenumber. The modal solution to (1) can be obtained for a rectangular element shown in Fig. 1, where D_x and D_y are dimensions of the rectangular element in the x- and y-directions, respectively.

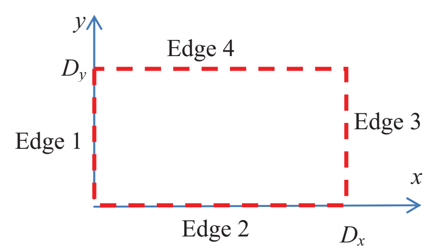

Fig. 1. A rectangular element.

Based on the modal solution to (1), the electric field inside the rectangular element can be expanded as

$$\vec{E}(x,y)=\sum_{i=1}^{4}\sum_{n=0}^{N_h}\vec{B}_{i,n}(x,y)E_{i,n}\ , \tag{2}$$

where

$$\vec{B}_{1,n}(x,y)=\frac{n\pi}{D_y}S_{xn}\cos[k_{xn}(D_x-x)]\sin\frac{n\pi y}{D_y}\hat{x}+ k_{xn}S_{xn}\sin[k_{xn}(D_x-x)]\cos\frac{n\pi y}{D_y}\hat{y}, \tag{3a}$$

$$\vec{B}_{2,n}(x,y)=k_{yn}S_{yn}\sin[k_{yn}(D_y-y)]\cos\frac{n\pi x}{D_x}\hat{x}+ \frac{n\pi}{D_x}S_{yn}\cos[k_{yn}(D_y-y)]\sin\frac{n\pi x}{D_x}\hat{y}, \tag{3b}$$

$$\vec{B}_{3,n}(x,y)=-\frac{n\pi}{D_y}S_{xn}\cos[k_{xn}x]\sin\frac{n\pi y}{D_y}\hat{x}+ k_{xn}S_{xn}\sin[k_{xn}x]\cos\frac{n\pi y}{D_y}\hat{y}, \tag{3c}$$

$$\vec{B}_{4,n}(x,y) = k_{yn} S_{yn} \sin[k_{yn} y] \cos\frac{n\pi x}{D_x}\hat{x} - \frac{n\pi}{D_x} S_{yn} \cos[k_{yn} y] \sin\frac{n\pi x}{D_x}, \quad (3d)$$

$$k_{xn} = \sqrt{k_c^2 - (n\pi/D_y)^2} \quad , k_{yn} = \sqrt{k_c^2 - (n\pi/D_x)^2} \,,$$

$$S_{\xi n} = \begin{cases} 1, \text{if } k_{\xi n} = s\pi / D_\xi \; (s \text{ is an integer}) \\ \csc(k_{\xi n} D_\xi) / k_{\xi n}, \text{otherwise} \end{cases} .$$

$S_{\xi n}$ is the normalization factor to ensure the continuity of tangential fields, where ξ can be *x* or *y*. $E_{i,n}$ is the *n*-th modal expansion coefficient for the tangential electric field along the *i*-th edge. It can be shown that basis functions in (3) have the following three properties. 1) It can be shown that $\nabla \cdot \vec{B}_i^n(x,y) = 0$. Namely, basis functions in (3) are divergence free; 2) The tangential electric field along the *i*- th edge of the rectangular element is only determined by $E_{i,n}$, which ensures the continuity of the tangential electric field; 3) The normal magnetic field derived from (2) satisfies the Helmholtz equation. The third property is important because it allows the element to be arbitrarily large. Equation (3) defines the macro basis function for one element. For multiple elements, the macro basis function may be defined on an edge. Fig. 2 illustrates two cases of edge directions. Depending on the direction of the *m*-th edge, the macro basis function can be defined as

$$\vec{B}'_{m,n}(x,y) = \begin{cases} \vec{B}_{4,n}^{m-}(x_m^-, y_m^-), \text{if } \hat{t}_m \times \hat{x} = 0 \text{ and } (x,y) \in \Omega_{m-} \\ \vec{B}_{2,n}^{m-}(x_m^+, y_m^+), \text{if } \hat{t}_m \times \hat{x} = 0 \text{ and } (x,y) \in \Omega_{m+} \\ \vec{B}_{3,n}^{m+}(x_m^-, y_m^-), \text{if } \hat{t}_m \times \hat{y} = 0 \text{ and } (x,y) \in \Omega_{m-} \\ \vec{B}_{1,n}^{m+}(x_m^+, y_m^+), \text{if } \hat{t}_m \times \hat{y} = 0 \text{ and } (x,y) \in \Omega_{m+} \end{cases}, \quad (4)$$

where $(x_m^\pm, y_m^\pm)$ is the local coordinate originated at the left and lower corners of $\Omega_{m\pm}$. $\hat{t}_m$ is the tangential vector along the *m*-th edge. The superscript $m\pm$ of $\vec{B}$ means the geometry parameters of $\Omega_{m\pm}$ is substituted in (3).

III. THE FINITE MACRO-ELEMENT METHOD

Using the macro basis function in (4), the electric field is expanded as

$$\vec{E}(x,y) = \sum_{m=0}^{M} \sum_{n=0}^{N_h} \vec{B}'_{m,n}(x,y) w_{m,n} \,, \quad (5)$$

where $w_{m,n}$ = 0 if the *m*-th edge falls on a boundary of perfect electric conductor. Substituting the field expansion into the following equation

$$\nabla_t \times \nabla_t \times \vec{E} - k_c^2 \vec{E} = 0 \,, \quad (6)$$

and applying the variational principle, the following matrix equation can be derived

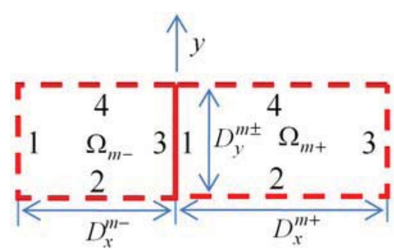

a.) y-directed edge.

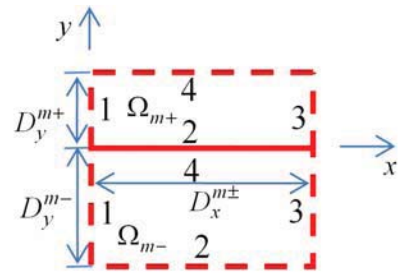

b.)x-directed edge.

Fig. 2 Two cases for the direction of the *m*-th edge.

$$\mathbf{Ax} = \mathbf{0} \,, \quad (7)$$

where

$$A_{i,j} = \iint_{\Omega_p} \nabla_t \times \vec{B}'_{p,q}(x,y) \cdot \nabla_t \times \vec{B}'_{m,n}(x,y) \, d\Omega - k_c^2 \iint_{\Omega_p} \vec{B}'_{p,q}(x,y) \cdot \vec{B}'_{m,n}(x,y) \, d\Omega, \quad (8)$$

$$i = p(N_h + 1) + q, \; j = m(N_h + 1) + n. \quad (9)$$

The integrands in the first term of (8) are inner product of the curls of macro basis functions. According to the definition of the macro basis function in (4), the curls of $\vec{B}'_{m,n}$ can be easily obtained from the curls of the basis functions defined in (3), which are

$$\nabla_t \times \vec{B}_{1,n}(x,y) = -k_c^2 S_{xn} \cos[k_{xn}(D_x - x)] \cos\frac{n\pi y}{D_y} \hat{z} \,, \quad (10a)$$

$$\nabla_t \times \vec{B}_{2,n}(x,y) = k_c^2 S_{yn} \cos[k_{yn}(D_y - y)] \cos\frac{n\pi x}{D_x} \hat{z} \,, \quad (10b)$$

$$\nabla_t \times \vec{B}_{3,n}(x,y) = k_c^2 S_{xn} \cos[k_{xn} x] \cos\frac{n\pi y}{D_y} \hat{z} \,, \quad (10c)$$

$$\nabla_t \times \vec{B}_{4,n}(x,y) = -k_c^2 S_{yn} \cos[k_{yn} y] \cos\frac{n\pi x}{D_x} \hat{z} \,. \quad (10d)$$

Depending on the local numbers of edges *p* and *q*, the integrands in (8) may take different forms. For all cases, the integrands can be simplified to product and sum of trigonometry functions and the integral can be computed analytically. Since there are many combinations of the four basis functions in (3), the expression for the elements of matrix **A** is very lengthy and it is omitted here. Once matrix **A** is available, the cutoff wavenumber k_c can be found by enforcing the determinant of matrix **A** to zero.

IV. Simulation Results

The cutoff wavelengths of double ridged and vaned waveguides are computed using the finite macro-element method. Their geometries are shown in the inset of Fig. 3, where the dashed lines are the edges of elements. Convergence behavior against N_h is plotted in Fig. 3, where errors are computed against results obtained with N_h=32. For the double ridged waveguide, very good accuracy can be obtained with N_h=1. On the other hand, N_h=7 should be used for the vaned waveguide. The convergence for the vaned waveguide is not as fast as the double ridged waveguide. This may be due to the field singularity near the vane edge, which should be dealt with using a different basis function. The cutoff wavelength of the dominant mode in the vaned waveguide is computed as the vane depth varies, and Fig. 4 compares results from different methods. It is seen that the proposed method provides good accuracy with coarse elements, which is highly desirable in modeling large and uniform structures.

V. Concluding Remarks

This paper has proposed a finite macro-element method for electromagnetic boundary-value problems. The modal solution to the Helmholtz equation has been used as the macro-basis function in the proposed method. Unlike conventional basis functions, the macro-basis function proposed in this paper automatically satisfies the Helmholtz equation, which allows a large element size. Simulation results have been presented to illustrate the advantages of the finite macro-element method. It has been observed that the finite macro-element method predicts the eigen-values of various waveguides accurately using very coarse elements. One limitation of the proposed method is the number of modal functions increases when field singularities exist. Future work includes combining the finite macro-element method with the conventional FEM to model structures with both regular and irregular geometries (e.g. a reverberation chamber).

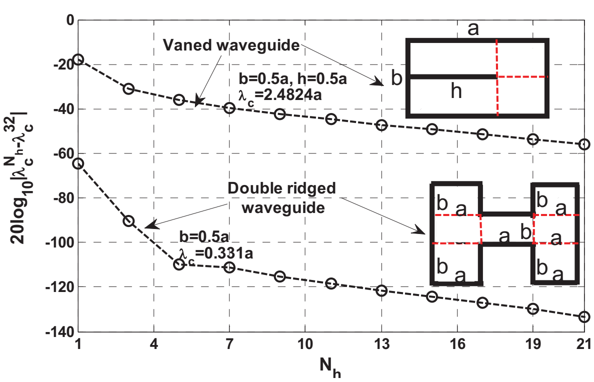

Fig. 3: Cutoff wavelength error against N_h.

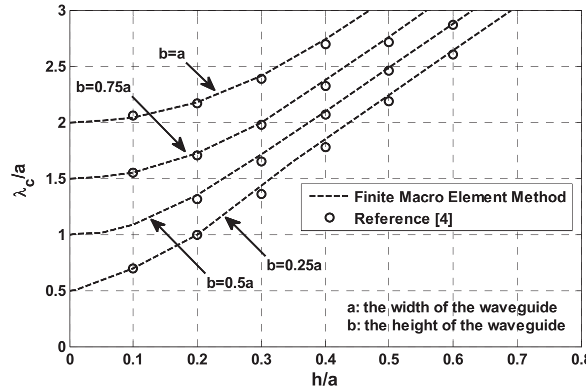

Fig. 4: Cutoff wavelength of vaned waveguide.

References

[1] J. Jin, *The Finite Element Method in Electromagentics*, NY: John Wiley & Sons, 1993.

[2] J. Liu and J. M. Jin, "A special higher order finite-element method for scattering by deep cavities," *IEEE Trans. Antennas Propagat.*, vol. 48, no. 5, pp. 694–703, May 2000.

[3] J. M. Jin, J. Liu, Z. Lou, and C. S. T. Liang, "A fully high-order finite-element simulation of scattering by deep cavities," *IEEE Trans. Antennas Propagat.*, vol. 51, no. 9, pp. 2420–2429, Sep. 2003.

[4] P. Silvester, "A general high-order finite-element waveguide analysis program," *IEEE Trans. Microwave Theory Tech.*, vol.17, pp. 204-210, Apr. 1969.